

SUBSURFACE CANAL SEEPAGE DETECTION USING RISAT-1 SAR DATA IN PARTS OF HANUMANGARH DISTRICT, RAJASTHAN

R. L. Mehta, T. Ahmad and A. Misra
MTDD/AMHTDG/EPISA, Space Applications Centre, ISRO, Ahmedabad-380015
rlmehta@sac.isro.gov.in

KEYWORDS: Dual (co and cross) polarisation, Multi-date images

ABSTRACT: Indira Gandhi Canal Project has enhanced considerable food production in desert area of Rajasthan, it also brought problems such as waterlogging and secondary salinisation. Impounding of Ghaggar flood water in natural depression is the main cause of seepage. Villages are located at lower altitude than the level of water stored in depressions, which creates a steep gradient and sand dunes being pervious, cause heavy seepage. Steady rise of water table cause water logging conditions in surrounding areas. The unlined canals from the saddle dams and continuous application of surface irrigation at higher frequencies have further added to the problem. One of the significant advantages of SAR is penetration through dry soil and detect subsurface geological and fluvial features. This paper presents the results of identifying subsurface canal seepage in the sand dune area of Hanumangarh district, Rajasthan using multi-date MRS RISAT-1 SAR data. Signature of high subsurface soil moisture accumulated in the depressions below the sand dunes and along the canal were analysed and identified as seepage areas. Landsat-8 images and field soil moisture data were used as complementary information to find the surface and subsurface soil moisture, crop and vegetation condition of the area. Subsurface moisture was identified with higher sensitivity in the cross polarizations (HV) images due to high volume scattering caused by the buried moisture bearing structures. Cross polarization ratio (CPR) observed was higher in case of subsurface soil moisture than surface moisture signature. Significant depletion in soil moisture of seepage areas was observed in the images acquired during the month of June, 2015.

INTRODUCTION

The Indira Gandhi Nahar Pariyojana (IGNP) occupies the north-western of the “Thar Desert” of Rajasthan State. It is one of the biggest projects of its kind in the world aiming at transforming desert wasteland into agriculturally productive area. The project covers the districts of Sri Ganganagar, Hanumangarh, Churu, Bikaner, Jaisalmer, Jodhpur and Barmer. It is comprising of culturable Command Area (CCA) of 19.63 lac ha and irrigated land of 15.17 lac ha (Mayur, 2017). Before the commencement of IGNP in 1963, Thar desert had absolute dependence upon uncertain rainfall and perpetual violent fluctuations in production of crops were common features and they put the agricultural activities to business of secondary importance. With the introduction of IGNP various factors like the absence of natural drainage and the presence of the hard pan at shallow depth, excessive intense irrigation and a certain amount of mismanagement of the canal water have all contributed collectively in creating many adverse environmental effects. Rise in water table, seepage, waterlogging, salinization, creation of marshy lands, invasion of obnoxious weeds and some related health hazards are the major ones among them. These effects are exercising a considerable impact on the entire ecology of the region. Waterlogging and salinization are the foremost among these problems. Waterlogging is a direct consequence of the rise in water table. The water table was very low in the area before the introduction of the canal irrigation. It ranged between 40 to 51m bgl in the year 1952. Now around 10.4% of the total irrigated area by the IGNP has a water table depth between 0 to 6 m. This rise in water table is caused by excessive intense irrigation, seepage from the canal and above all by the presence of hard pan at a low depth of 0 to 20 m. When the water table rises up to 6 m bgl, the area is considered potentially sensitive area in respect of the waterlogging. The area of Stage-I of IGNP has been facing the problems of waterlogging and secondary soil salinization by the year 2000. During the period 1999 to 2003, the waterlogged, critical and potentially sensitive areas have shrunken considerably (Mayur, 2017). Ground water elevation has declined in the areas around Tibi, Chistian, Suratgarh, Anupgarh and Sattasar in the year 2010 as compared to 2000 as result of remedial measures taken to combat water logging as per the recommendations of conjunctive studies carried out by Central Ground Water Board (CGWB), Manoj et.al., 2013.

It has been shown that there is a wide range of applications for satellite imaging radar products. Furthermore, ongoing research and development is continually expanding the current range of applications. One of the significant capability of SAR is penetration in dry soil and detection of subsurface geological, fluvial and archaeological features. Radar penetration has attracted extensive attention since SIR-A revealed subsurface relict old valley in Selima sand sheet of eastern Sahara in 1982. The penetration depth of microwave is defined as the

depth (dp) when the electric field intensity attenuates to $1/e$ of its incident value in a dielectric media. The penetration depth is in direct proportion to wavelength, and in inverse proportion to complex dielectric constant for natural loose media. Complex dielectric constant is mainly related to water content of the material.

Over arid areas, L-band SAR can explore the subsurface down to several meters when covered by dry material such as sand (Schaber et al. 1986, Paillou et al., 2003, Williams and Greeley, 2001 and McCauley, 1982). Using SIR-A data, Schaber et al. 1986 estimated the penetration depth of L-band SAR to be 1.5 m through sandy sediments in the southern desert of Egypt. Based on SIR-B, other studies discussed L-band radar penetration capabilities in Saudi Arabia (Berlin et al., 1986) and in the Nevada desert (Farr et al., 1986) to reveal buried scatterers. More recently, other authors showed the ability of multi-frequency and polarimetric SAR to map subsurface geology below sandy material (Abdelsalam et al., 2000, Dabbagh et al., 1997, Rajawat, 2008, Rajawat et al., 2003 and Schaber et al., 1997).

Many experiments demonstrated that low frequency radar has good penetration capability especially under dry soil condition. Guo Huadong (1996) led his team to carry out radar penetration experiment in Alxa Plateau. Corner reflectors were buried under sand. This experiment proved that the maximum penetration depth of L-band wave in dry sand can reach up to 2.82 m and the penetration depth is in inverse proportion to water content of sand. In the field survey, it was found that there were some wet sands with 46% of water in tens of centimetres under the dry ground surface. This also suggested that, in case of buried sand with high moisture content, the L band penetration can reach up to one meter depth. This effect will enhance the backscattering response from the subsurface interface. Elachi et al., 1984 in a study proved that with an increased incidence angle ($>30^\circ$), the backscattering response from subsurface interface was enhanced due to more refraction from air-sand interface. In this study subsurface seepage areas were identified. Signatures of high surface soil moisture areas and that of subsurface seepage areas were compared. Optical data were used to find the crop, vegetation and surface moisture condition.

STUDY AREA

This study was taken up covering parts of Hanumangarh district of Rajasthan (Fig. 1). It is northernmost district with a total geographical area of 9,70,315 ha, located between $28^\circ46'30''$ to $29^\circ57'20''$ north latitude and between $73^\circ49'55''$ to $75^\circ31'32''$ east longitude. It is surrounded by Ganganagar district in the west, Bikaner and Churu districts towards south west and south; Sirsa district of Haryana in the east and Ferozepur district of Punjab in the north. Location map of study area is shown in Figure 1. The district came into existence as 31st district of Rajasthan on 12th July, 1994 by bifurcation of Ganganagar district. The introduction of canal irrigation through Indira Gandhi Nahar Project (IGNP) in the hot arid ecosystem of northern Rajasthan has completely changed the land use scenario by putting more than 33 % area of the Hanumangarh district into irrigated farming with cotton wheat cropping system.

The climate of the study area is semi-arid to arid except southwest monsoon season during the period June to mid of September, which is followed by post monsoon period till the end of November. The winter season is from December to February and is followed by summer from March to June. The mean daily maximum temperature varies from 20.5°C during January to 42.2°C during June while mean daily minimum temperature in the district varies from 4.7°C during January to 28.1°C during July. The Normal Annual Rainfall of the district during the period 1901-2006 has been 333.27 mm. The district is a part of Thar desert and is covered by thick layer of alluvium and wind-blown sand. Generally sand dunes are 4 to 5 m in height. Regional elevation of ground ranges from 100 to 300 metres above mean sea level (msl). The district has a regional slope of less than 5 m/km. Ghaggar river, locally known as Nali, is the only marked surface water drainage, which flows from NE to SW. It is an ephemeral river which sometimes gets flooded during monsoon.

The study area is a part of IGNP command area Stage-I and irrigated by Rawatsar and Naurangdesar distributaries. The problem of waterlogging and surface ponding has destroyed the natural environment of the area and has caused formation of the saline soils. The monitoring of observation wells and piezometer indicates that the water table in the area is rising at an average rate of 0.93 m per year from the year 1952-1994. In general, a rise of 0.40 m per year for the period 1952-1970, 0.66 m/year for the period 1984-1989 and 0.41 m/year for the period 1995-2004 has been recorded in waterlogged areas (Mayur, 2017).

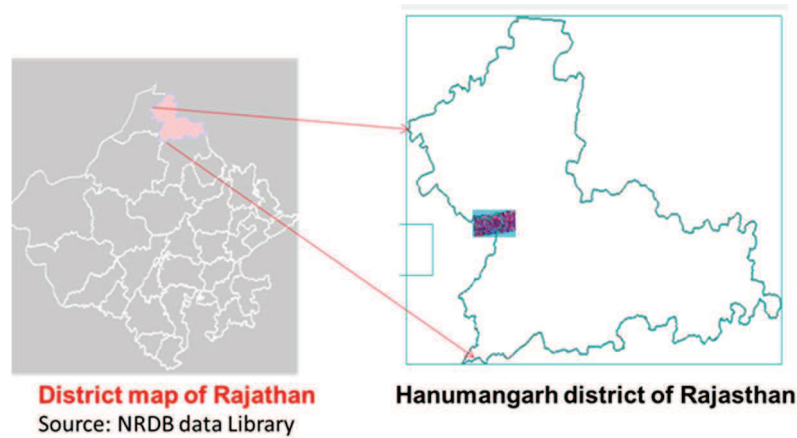


Figure 1: Location map of the study area

MATERIALS AND METHODS

The methodology included extraction of dual polarisation C-band RISAT (MRS) data. The enhanced Lee filter with 5x5 kernel window size was used for speckle suppression. The data were converted to backscattering coefficient domain using the following equation.

$$\sigma_0(\text{dB}) = 20 * \log_{10}(\text{DN}_p) - K_{\text{dB}} + 10 \log_{10} \left(\frac{\text{Sin}(i_p)}{\text{Sin}(i_{\text{center}})} \right) \quad (1)$$

Where,

σ^0 = radar backscatter coefficient in dB

DN_p = digital number or the image pixel gray-level count for the pixel p

K_{dB} = calibration constant in dB

i_p = incidence angle for the pixel position p (in degree)

i_{center} = incidence angle at the scene center (can be obtained from BAND_META.txt file)

Image registration with optical data was done by selecting the GCPs in both the images. Signatures of high soil moisture at surface and subsurface were compared using the dual polarization SAR data. Subsurface moisture was detected as greenish tone in dual polarisation image of summer season. Data processing and signature analysis was performed using the ENVI software. Visual interpretation technique was used in identifying canal seepage areas under the sand dunes and along the unlined canals. Multi-date images procured during 2015 and 2016 were used to study the temporal sub-surface soil moisture variations. The list of images used in the study is given in table 1. Main steps of methodology followed are given in figure 2. Radiometrically corrected Landsat-8 images acquired on 21st March, 2015 and 22nd Apr., 2015 along with ground truth measurements of surface and subsurface soil moisture were used as complementary information to find the crop and vegetation cover and soil moisture condition in the study area.

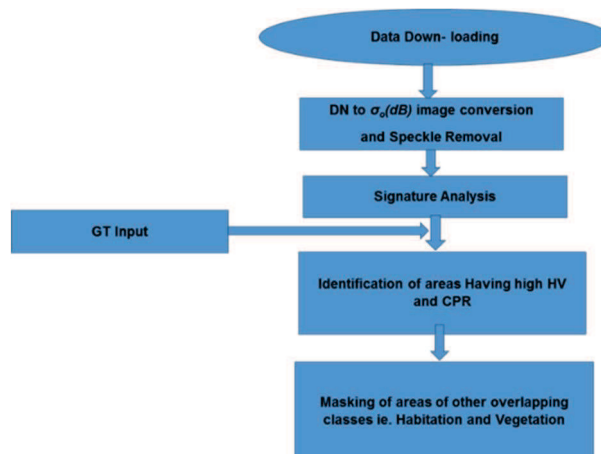


Figure 2: Flow chart of methodology

Table 1: Details of the Satellite data used.

Satellite / Mode	Polarisation	Date of Acquisition	Incidence angle at Centre (deg.)	Resolution (m)
RISAT-1 / MRS	Dual (HH, HV)	31 May, 2014 5 th Feb., 2015 21 st Apr., 2015 16 th May, 2015 07 th Nov., 2015 23 rd Jun, 2015 5 th Apr., 2016 7 th Jun., 2016	35 to 40	18
Sentinel-1A	Dual (VV, VH)	18 th Mar, 2017 11 th Apr., 2017 05 May, 2017 10 th Jun., 2017	35 to 40	10
Landsat-8		21 st Mar., 2015 22 nd Apr., 2015		30

RESULTS AND DISCUSSIONS

Impounding of Ghaggar flood water in natural depression is the main cause of seepage. Villages are located at lower altitude than the level of water stored in depressions, which creates a steep gradient and sand dunes being pervious and cause heavy seepage. Excessive irrigation, canal seepage from the main canal, distributary unlined canals and absence of natural drainages add up the problem (Fig. 3). Seepage water start accumulating on impervious calcareous or gypsum layers and water table rises towards the surface and may resulted into waterlogging/ salinity hazard (Fig. 4) in the area. The productivity of the waterlogged land especially crop yields declined substantially leading the farmers to quit their occupation.

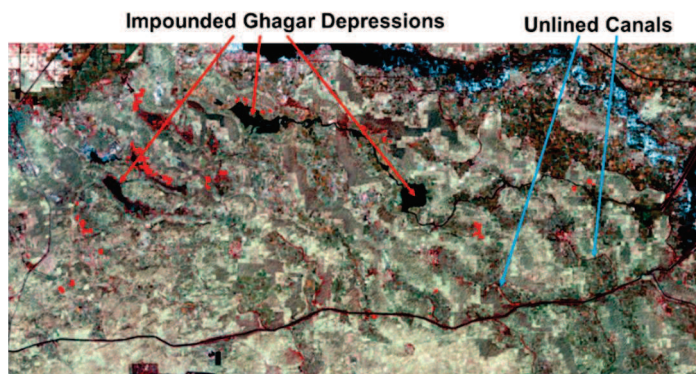


Figure 3: Main sources of seepage in the study area (Landsat-8, 22nd Apr., 2015)



Figure 4: Field photographs showing sub-surface seepage and water-logging/ Salinity.

Subsurface penetration capability of SAR can be used to map subsurface heterogeneities such as geological interfaces or wet soil layers. As regards with surface soil moisture, it is well known that the presence of water influences the radar response of a terrain. Experiment and theoretical studies, based on empirical or semi-empirical models, have revealed this phenomenon. The surface soil moisture variations can be easily modelled using co-polarisations HH, VV images (Dubois et al., 1995, Shi et al., 1997). In principle both the surface and volume scattering are present in scattering from bare soil (Ulaby et al., 1982). In the surface scattering, the backscattering is proportional to the relative complex dielectric constant of the surface and its angular scattering pattern is governed by the surface roughness. In volume scattering, the scattering strength is proportional to the dielectric discontinuities and their densities inside the medium (below the surface) angular scattering pattern is determined mainly by the roughness of the boundary surface roughness. In general, the spatial locations of these dielectric discontinuities are random, the wave scatter within the volume in all directions resulting to volume scattering. In case the upper layer is very thick and sandy, it will have negligible contribution toward the total scattering.

Because pure volume scattering occurring in the upper sand layer appears to be weak since the material is homogeneous and has low permittivity (Trough, 1995). Grandjean et al., 2001 recognised subsurface high moisture paleosoil under a sand dune using L-band airborne polarimetric SAR data. Co-polarised signal contains both surface and non surface scattering components, whereas cross polarized signal is composed of mainly non surface i.e., subsurface and volume scattering components. A high backscattering from linear subsurface moisture bearing structure (drain) contrasting to dark tone of the dry sand dune was attributed to strong depolarisation of incident wave resulting in significant cross polarization return. Because they behave like moisture tanks.

The MRS dual polarisation image acquired on 21st Apr., 2015 displayed as HH:HV:HH in red, green and blue color, respectively is showing canal seepage areas under the sand dunes (Figure 5a). High subsurface soil moisture under the pervious sand dunes resulted in higher backscattering in cross polarisation (HV) due to volume scattering and appeared in green tone. While no seepage areas due to low moisture condition in both the polarisation (HH and HV) appeared in dark tone due to specular reflection and no volume scattering contribution from the subsurface layer. Fig. 5b is a standard Landsat-8 image (22nd Apr., 2015) of the study area procured within time difference of one day to that of SAR image. Inter-dunal flat dry areas are seen in whitish tone due to high reflectance of sand. Undulating elevated dunes of around 2 to 4m height are represented by light greenish tone on the Landsat-8 FCC. Subsurface soil moisture cannot be detected using Landsat image due to the fact that optical wave cannot penetrate into the soil medium and used only for the surface moisture condition assessment. All sand dunes with canal seepage as well as without canal seepage attributed the same light greenish signature tone.

The canal seepage as observed in the HH polarization image appeared in darker tone and showed a small difference in backscattering of canal seepage and non-seepage areas, though co-polarisations are considered best for surface soil moisture estimation (Fig. 6a). The sub-surface seepage areas appeared in very bright tone in cross polarisation (HV) image (Fig. 6b) due to high volume scattering from sub-surface moist soil. The image (HV) attributed a large variation in backscattering from seepage and non-seepage areas showing a high sensitivity to subsurface soil moisture variations. The inter-dunal flat which are not affected by seepage were observed in darker tone in both the polarisations. Thus, sub-surface moisture due to capillary rise from the shallow water table areas could be easily detected in the cross polarisation image. This was due to the fact that pure volume scattering due to the dielectric discontinuity in the upper dry sand layer and moist sub-soil layer resulted in the strong volume scattering (Grandjean et al., 2001), while contribution of surface scattering represented by co-polarizations was poor from both the soil layers. Also, dry sandy soil of the desert is more suitable condition for wave penetration into the soil medium (Ulaby et al., 1986).

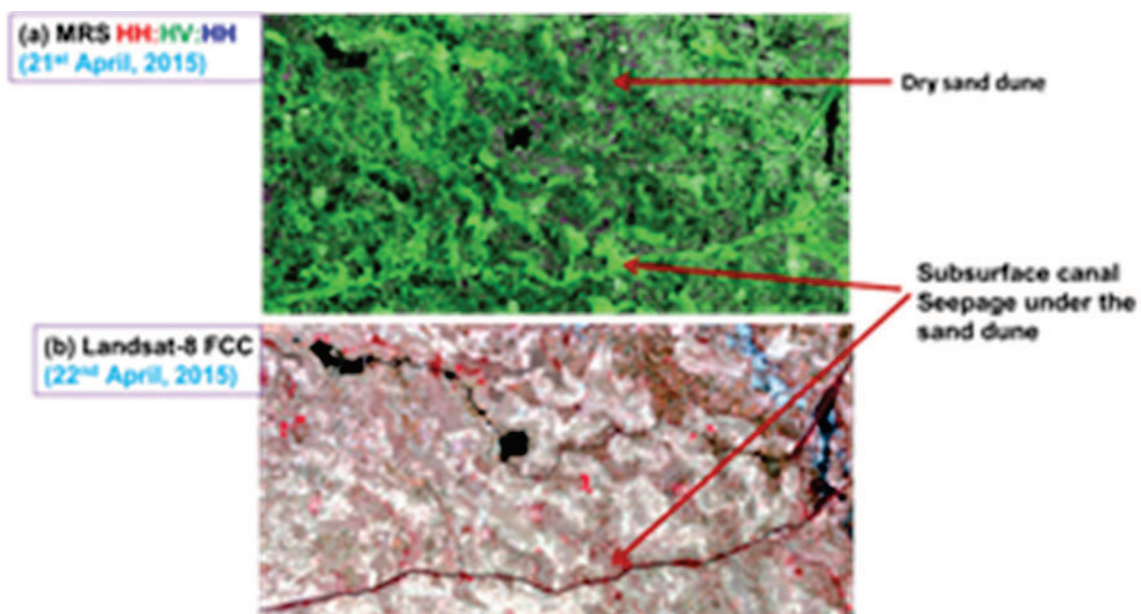


Figure 5: Dual Polarization, C-band MRS RISAT-1 image (21st April, 2015) showing canal seepage under the sand dune

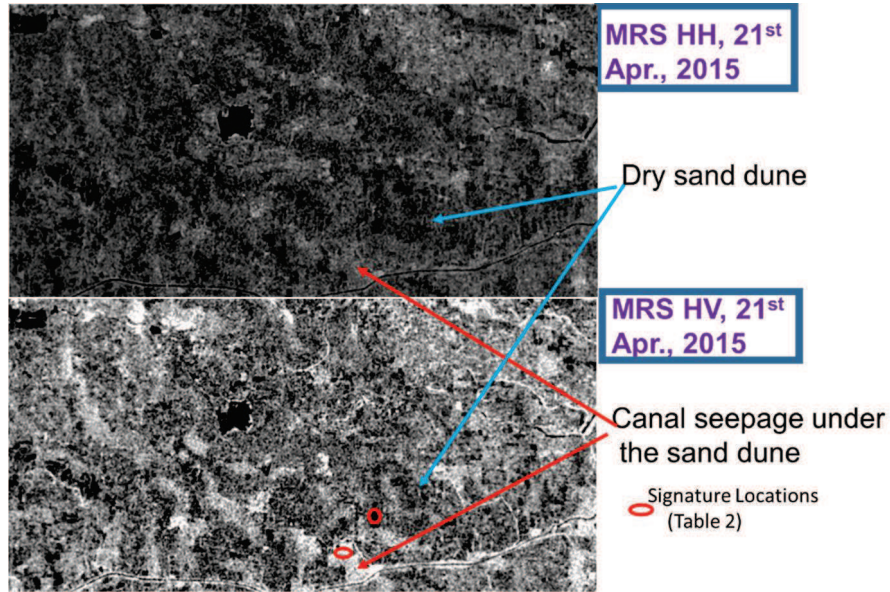


Figure 6: (a, upper) MRS RISAT-1 HH and (b, lower) HV polarization images (21st April, 2015). Cross polarization (HV) image showing higher sensitivity to canal seepage under the sand dunes

Image signatures collected from high surface soil moisture area, perched condition sub-surface moist area and dry soil were analysed. Represented locations for perched condition sub-surface moist area and dry soil are marked on Fig. 6b. Best dry condition signature was observed in the month of June. For high surface soil moisture area represented location is not covered in any of the figures, but the coordinate were 30° 6'50" and 73° 44' 31" of the MRS image procured on 21st Apr., 2015. For surface soil moisture HH polarisation signature variation was -18.40 dB to -5.81 dB and HV was -25.32 dB to -17.33 dB for low and high surface soil moisture, respectively (Table 1). This showed a high sensitivity (12.59 db) of HH polarisation for surface soil moisture estimation. In case of sub-surface soil moisture estimation, HH polarisation signature variation was -18.40 dB to -11.80 dB and HV was -25.32 dB to -17.55 dB in case of low and high moisture, respectively (Table 2). This showed a higher sensitivity (7.77 db) of HV polarisation for sub-surface soil moisture estimation.

In surface soil moisture, cross polarization ratio (CPR) observed was -11.52 dB in comparison to -5.75 dB in the case of subsurface soil moisture signature. A significant higher cross polarization ratio indicated presence of subsurface soil moisture due to seepage from adjoining canal. This increase in cross polarization (HV) and CPR was due to dominating volume scattering from sand covered fluvial feature as compared to surface scattering from soil surface. Buried moisture structures behave like moisture tank and result into depolarization and high backscattering due to volume scattering. Though, surface soil moisture is sensitive to co-polarizations. Cross polarization (HV) and CPR were observed as useful parameters to distinguish subsurface soil moisture in contrast to high sensitivity of co-polarisation (HH) to surface soil moisture estimation.

Table 2 : Co and cross polarisation signatures under different soil moisture conditions

		HH	HV	HV/HH (Cross Pol. Ratio)
High surface soil moisture	σ° (dB)	-5.81	-17.33	-11.52
	S.D.	1.66	1.25	1.54
High soil moisture (perched condition)	σ° (dB)	-11.80	-17.55	-5.75
	S.D.	1.05	1.12	1.23
Low soil moisture	σ° (dB)	-18.40	-25.32	-6.92
	S.D.	1.07	0.72	1.09

Temporal MRS images were studied to find out the temporal variations in seepage signatures. A small variation was observed in signatures of different months. Changes in signatures are mainly due to amount of surface and subsurface soil moisture and proportion of crop cover. Surface moisture and crop cover reduce SAR penetration into soil medium. However, volume scattering from subsurface layers depends upon the dielectric discontinuities between dry surface and moist subsurface layer. Highest decrease of 1 to 3 dB was observed in the image acquired on 23rd June, 2017 (Fig. 7) in comparison to 21st April, 2015 image due to depletion of soil moisture in the summer season. An increase in canal seepage was detected in the Sentinel image procured on 16th June, 2017 when the canal was full of water, in comparison to image of 10th April, 2017 when the water supply was closed in the canal from 27th Mar., to 16th April, 2017 for a repair work (Fig. 8).

MRS RISAT-1 SAR data acquired during winter season (5th Feb., 2015) and during summer season (21st April, 2015) showed that water bearing structures i.e. water courses could be easily detected in case of summer season images than the winter season (Fig. 9). Water spread through seepage on both sides of the unlined canals resulting in higher width of canal than observed in optical image. During summer season upper layer is dried, volume scattering from the lower moist soil makes the identification of water courses easy. Most of these features could not be identified in the optical image due to no penetration of wave into the soil medium. An integrated image prepared using images procured on 21st April 2015, 4th May, 2017 and 23rd June, 2015 demonstrated that water courses could be delineable up to a longer length than observed in the Landsat image (Fig. 10). This was possible due to SAR penetration in to the dry sand dunes and received volume scattering signal from the subsurface moist soil layer.

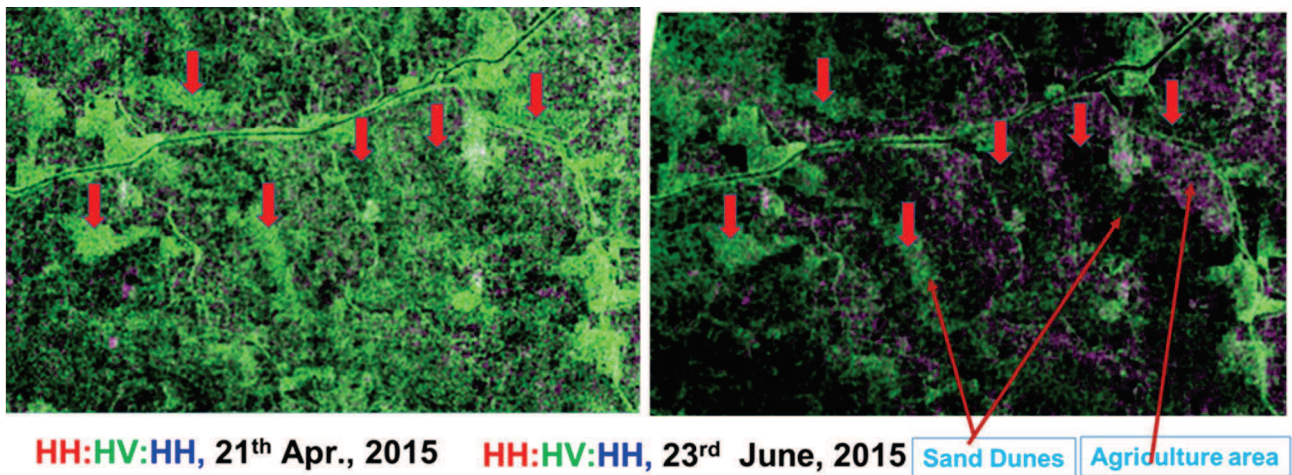


Figure 7: June image showing a depletion in seepage water (Green and Dark Tone) in the sand dunes

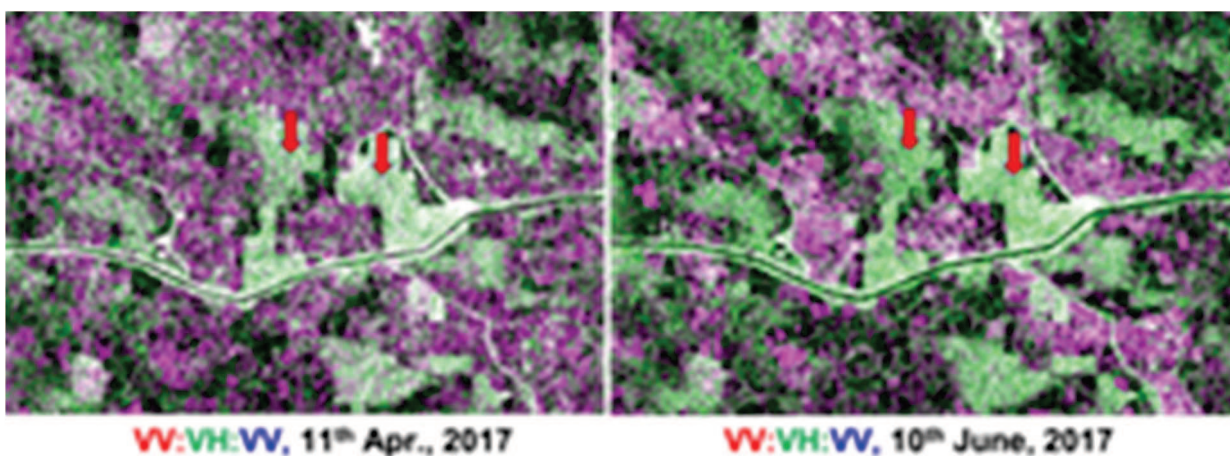


Figure 8: 11th June Sentinel SAR image is showing higher seepage (Green tone) as the canal is full of water as compared to the 10th Apr., 2017 image when the water supply was closed (from 27th Mar., 2017 to 16th Apr., 2017) for canal repair work.

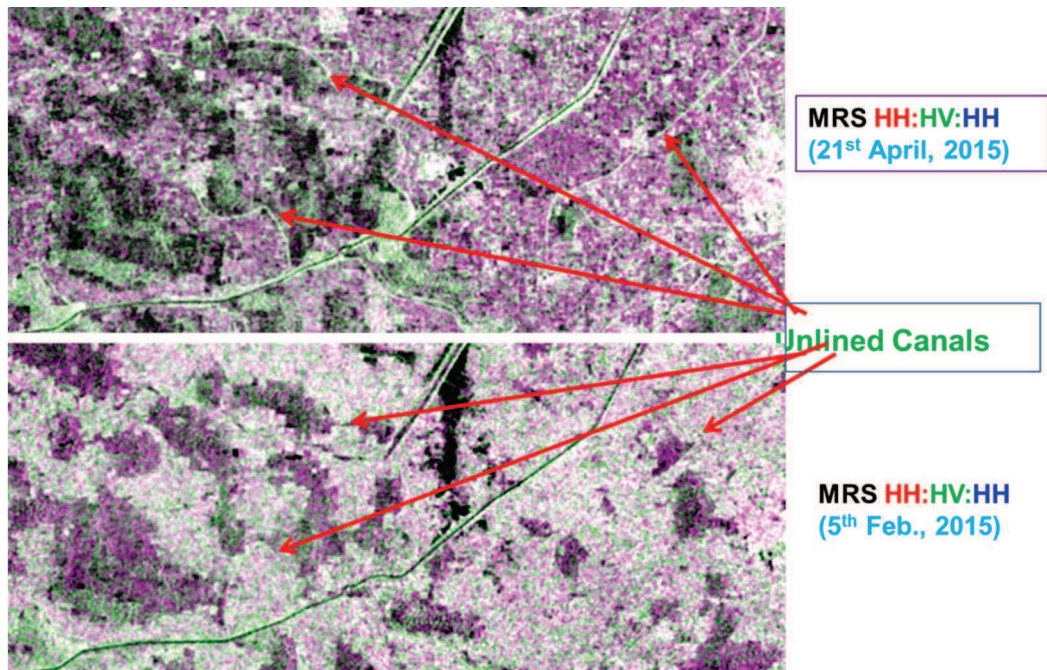


Figure 9: Summer season image (21st Apr., 2015) showing better delineation of unlined Canals as compared to winter season (5th Feb., 2015)

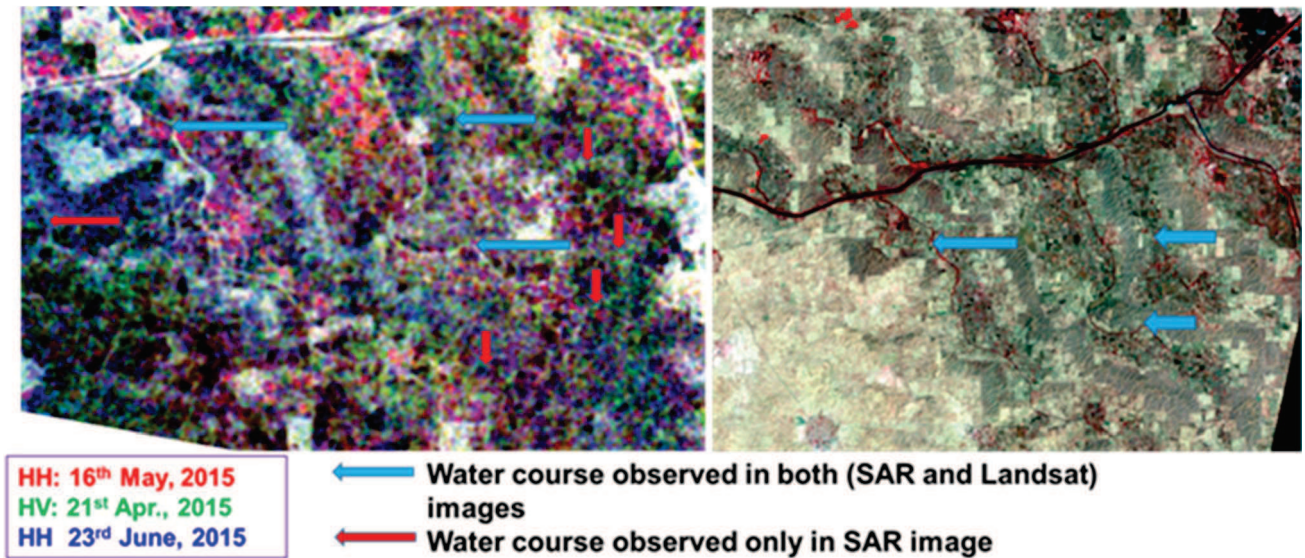


Figure 10: Multi-date Cross polarisation (HV) integrated image showing longer delineation of water courses compared to Landsat-8 image (22nd Apr., 2015)

IV CONCLUSIONS

The study was taken up to assess the potential of C-band dual polarization RISAT-1 MRS SAR data to identify the subsurface canal seepage areas. The main advantage of using SAR in desert terrain is that of high signal penetration during summer due to dry sandy soil surface. Also, the roughness effect is minimum due to smoothness in sandy soil surface. C-band SAR amplitude images were found very useful in discrimination of sand covered hydrological features. Following conclusions were drawn from this SAR and optical data analysis.

- Subsurface canal seepage can be successfully detected in the desert terrain using dual polarised C_band SAR image.
- Subsurface moisture was detected with higher sensitivity using cross polarization (HV) image than in co-polarization (HH) due to high volume scattering from the buried moisture structures.
- Cross polarization ratio observed was very high in case of subsurface soil moisture than surface and is a useful parameter for its detection.
- An analysis of summer and winter month images revealed that subsurface canal seepage was better detected in summer due to more SAR penetration in dry sand. Variation observed in temporal signatures of seepage areas is mainly attributed to surface soil moisture content, thickness of upper dry layer and quantity of subsurface moisture. Highest depletion in soil moisture of seepage areas was observed in 23rd June, 2015 image.
- Water courses having sub-surface moisture could be delineated up to longer length in summer months due to SAR penetration.

REFERENCES

- Abdelsalam, M. G., Robinson, C., El-Baz, F. and Stern, R. J., 2000. Applications of orbital imaging radar for geologic studies in arid regions: The Saharan testimony. *Photogrammetric Engineering and Remote Sensing*, 66 (6), 717-726.
- Berlin, G.L., M.A., Tarabzouni, A. Al-Nasser, K.M. Sheikho, and R.W. Larson, 1986. SIR-B Subsurface Imaging of a Sand buried Landscape: Al Labbah Plateau, Saudi Arabia. *IEEE Trans. Geoscience and Remote Sensing*, 24, 595-602.
- Dabbagh, A. E., Al-Hinai, K. G., Asif Khan, M., 1997. Detection of Sand-Covered Geologic Features in the Arabian Peninsula Using SIR-C/X-SAR Data. *Remote Sens. Environ*, 59, 375-382.
- Dubois, P.C., Van Zyl, J. and Engman E.T., 1995. Measuring soil moisture with imaging Radar, *IEEE Transactions on Geoscience and Remote Sensing*, 33, 915-926.
- Elachi, C., Roth, L.E., and Schaber, G.G., 1984. Spaceborne radar subsurface imaging in hyperarid regions. *IEEE Trans. Geosci. Remote Sensing*, 22, 383-388.
- Farr, T. G., Elachi, C., Hartl, P. H., and Chowdhury, K., 1986. Microwave penetration and attenuation in desert soil: A field experiment with the Shuttle Imaging Radar, *IEEE Trans. Geosci. Remote Sensing*, 24, 590-594.
- Grandjean G., P. Paillou, P. Dubois, T. Bernex, N. Baghdadi and J. Achache, 2001. Subsurface structure detection by combining L-band polarimetric SAR and GPR data: Example of the Pyla dune (France). *IEEE transaction on geosciences and remote sensing*, 39 (6), June 2001, 1245-1258.
- Guo Huadong, Zhu Liangpu, Shao Yun, 1996. Detection of structural and lithological features underneath vegetation canopy using SIR-C/X-SAR data in Zhao Qing test site of southern China. *Journal of Geophysical Research*, 101(E10), 23101.
- Manoj Shrivastava, I. K. Sharma and D. D. Sharma, 2013. Ground water scenario in Indira Gandhi Nahar, Pariyojna (IGNP) in parts of Sri Ganganagar, Hanumangarh, Churu, Bikaner, Jaisalmer, Jodhpur and Barmer districts, Rajasthan. *Memoir Geological Society of India*, no.82, 2013, 16-35
- Maurya, A, 2017. Study of waterlogging and soil salinization problem in and around Rawatsar Tehsil, Hanumangarh District in The command area of Indira Gandhi Nahar Pariyojna (IGNP) stage-I, Rajasthan, India, *International Journal of innovative research and advanced studies. IJIRAS*, Volume 4 Issue 4, 118-126.
- McCauley, J., Schaber, F., Breed, C. S., Grolier, M. J., Haynes, C. V., Issawa, B., Elachi, C. & Blom, R., 1982. Subsurface valleys and geo-archeology of the eastern Sahara revealed by Shuttle radar. *Science*, 318, 1004-1020.
- Paillou, P., Rosenqvist, A., 2003. The SAHARASAR project: Potential support to water prospecting in arid Africa by SAR. *Geoscience and Remote Sensing Symposium, IGRASS'03 Proceedings. IEEE International*, 3, 1493-1495.
- Rajawat, A.S., 2008. Identification of buried channel using fine beam RADARSAT SAR data for archaeological exploration in the Talakadu region, Karnataka, *SAC Courier*, 32 (3), 10-11.

- Rajawat, A.S., Verma, P.K. and Shailesh Nayak, 2003. Reconstruction of palaeodrainage network in northwest India: Retrospect and prospects of remote sensing based studies; Proc. Indian National Science academy; 69 A (2), pp.217-230.
- Schaber, G. G., McCauley, J. F., Breed, C. S., 1997. The use of multifrequency and polarimetric SIR-C/X-SAR data in geologic studies of Bir Safsaf, Egypt. Remote Sens. Environ., 59, 337-363.
- Schaber, G. G., McCauley, J. F., Breed, C. S., Olhoeft, G. R., 1986. Shuttle imaging radar: physical controls on signal penetration and subsurface scattering in the eastern Sahara. IEEE Trans. Geosci. Remote Sensing, 24, 603-623.
- Shi, J., Wang, J., Hsu, A.Y., O'Neill, P.E. and Engman, E.T., 1997. Estimation of bare surface soil moisture and surface roughness parameter using L-band SAR image data. IEEE Trans. Geosci. Remote Sensing 35, 1254-1266.
- Trouch, P.A., Vandersteene, Z. SU, Hoeben, R. and Wuethrich, M, 1995, Estimating microwave observation depth in bare soil through multi-frequency scatterometry, Laboratory of Hydrology and water management, University of Gent Coupure Links Gent, Belgium.
- Ulaby, F. T., Moore, R. K. and Fung. A. K., 1986. Microwave Remote Sensing: Active and Passive; From Theory to Applications: Volume-III, Artech House, Inc.
- Ulaby, F.T., M.K. Moore and A.K. Fung, 1982. Microwave Remote Sensing, Active and Passive. Norwood, MA: Artech House, Inc.
- Williams., K. K., Greeley, R., 2001. Radar Attenuation by Sand: Laboratory Measurements of Radar Transmission. IEEE Trans. Geosci. Remote Sens. GE-39:2521-2526.